DALTON
FULL PAPER

# Luminescent and redox-active ruthenium(II) and osmium(II) complexes with a rigid allene-bridged polyphosphine †

**Bo Hong,* Steven R. Woodcock, Sylvia K. Saito, Jeffrey V. Ortega**

*Department of Chemistry, University of California, Irvine, CA 92697-2025, USA*

A series of monometallic and homo- and hetero-bimetallic $Ru^{II}$ and $Os^{II}$ complexes with the polyphosphines 1,1′-bis(diphenylphosphino)ethene (bppe) and 1,1′,3,3′-tetrakis(diphenylphosphino)allene (tppa) have been prepared and characterized by $^{31}P$-{$^{1}H$} NMR spectroscopy, elemental analysis and fast atom bombardment mass spectral analysis. Their ground-state properties (including electrochemical behavior and electronic absorption) and excited-state properties (including luminescence, quantum yields and MLCT excited state lifetimes) are reported herein. All complexes exhibit room-temperature luminescence, with long-lived $^{3}$MLCT excited states observed for monometallic and homobimetallic $Os^{II}$ complexes with both bppe and tppa ligands. In the heterobimetallic $Ru^{II}$–$Os^{II}$ complex $[Ru(bpy)_2(\mu\text{-tppa})Os(bpy)_2][PF_6]$ (bpy = 2,2′-bipyridine) the luminescence of the $Ru(bpy)_2$-based unit is quenched by the connected $Os(bpy)_2$-based unit *via* energy transfer across the tppa spacer containing the allene bridge. Two overlapping one-electron oxidations, corresponding to the two $M^{II}$-based moieties (M = Ru or Os) bridged by the tppa spacer, are observed in the homobimetallic complexes.

The construction of low-dimensional artificial supramolecular systems from a discrete number of molecular components has been an area of ongoing interest.[1] Through the linkage of various prefabricated molecular components with light-related properties, photochemical molecular systems have been obtained to study the luminescence and redox properties, and intramolecular electron/energy transfer processes.[1–4] These systems will include several representative features. Synthetically we must have control of the choice, orientation and spacing of auxiliary ligand, donor/acceptor and spacer. To ensure the directionality and also construct multicomponent supramolecular systems with well defined structures, rigid spacers must be used to afford restricted conformational mobility and controllable distances between structural subunits. In addition, we must also have means to identify the mode and mechanism of energy or electron transfer as well as the electronic interaction between subunits spanned by spacers.

The role of spacers in such systems can be multifaceted; spacers can serve as conducting components to promote long range electronic communication and photoinduced electron/energy transfer, or as passive connecting components. In our search for suitable systems, we found that polyphosphines with rigid sp hybridized cumulenic carbon chains ($C_n$) are ideal candidates due to their rigidity, co-ordination versatility, and chemical/photochemical stability upon formation of various metal complexes.[5] Despite their versatile applications as complexing ligands,[5,6] polyphosphines have been much less incorporated in the construction of photochemical molecular systems when compared with N-containing ligands,[7] especially polypyridines. The use of phosphine groups in spacers provides two advantages. First, they can serve as linkage components between the $C_n$ chains and metal centers. Second, it has been reported[8–10] that the incorporation of phosphines in the polypyridyl–osmium(II) complexes can enhance the lifetimes of $^{3}$MLCT states.

In this paper, we report the synthesis, characterization and photophysical studies of monometallic (**2a** and **2b**) and bimetallic (**2c**–**2e**) ruthenium(II) and osmium(II) complexes of a specific tetratopic phosphine, namely, 1,1′,3,3′-tetrakis(diphenylphosphino)allene (tppa) with an unsaturated $C_3$ chain. Comparison of the redox chemistry and excited properties of these complexes with the analogous monometallic complexes (**1a** and **1b**) of 1,1′-bis(diphenylphosphino)ethene (bppe) will be carried out. Electronic absorption, steady-state and time-resolved emission spectroscopy have been used to study the ground-state absorption and redox properties, the excited-state decay kinetics, and the energy-transfer process in this system. The $^{3}$MLCT excited-state quantum yields and lifetimes of bimetallic complexes **2c**–**2e** are compared with the corresponding monometallic model complexes **2a** and **2b**, and the observed rate constant of energy transfer is estimated, from the MLCT excited-state lifetimes, for the structurally rigid and fixed bimetallic complex **2e**.

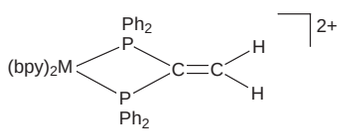


M = Ru **1a**, Os **1b**

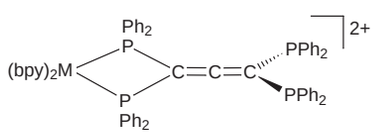


M = Ru **2a**, Os **2b**

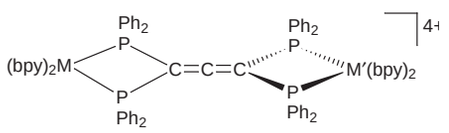


M, M′ = Ru **2c**, Os **2d**
M = Ru, M′ = Os **2e**

## Results and Discussion

### Synthetic routes

The preparation of monometallic and bimetallic complexes in this study reveals several interesting reactivity patterns. For any metal center, the polyphosphines bppe and tppa can coordinate in a bis(chelating) mode or serve as a monodentate ligand. An extended reaction time is required in order to obtain

† *Non-SI unit employed*: eV ≈ $1.602 \times 10^{-19}$ J.

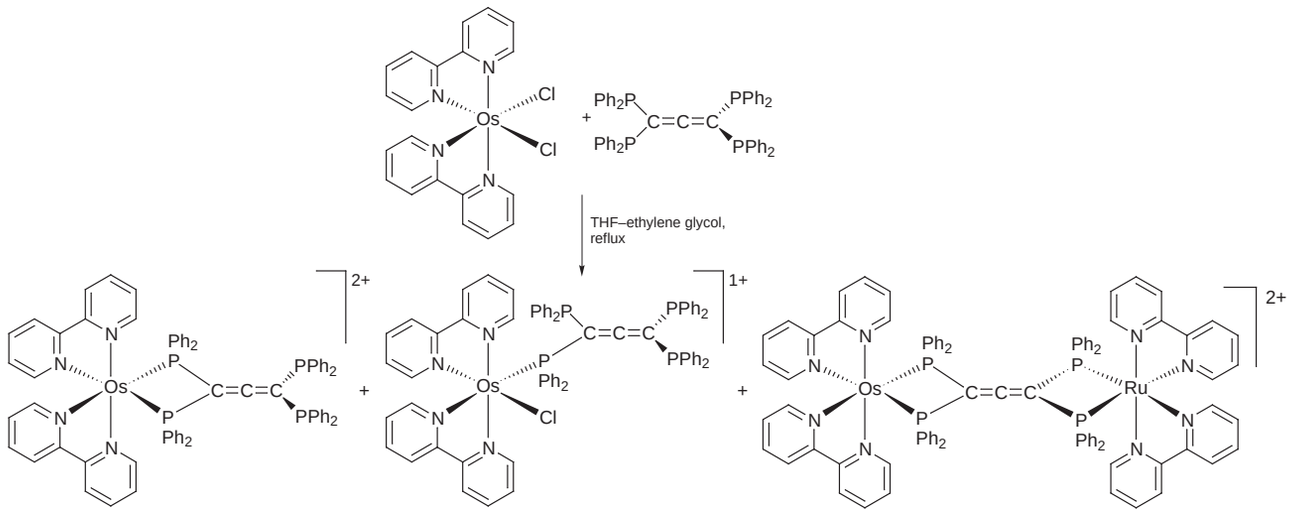


**Scheme 1**

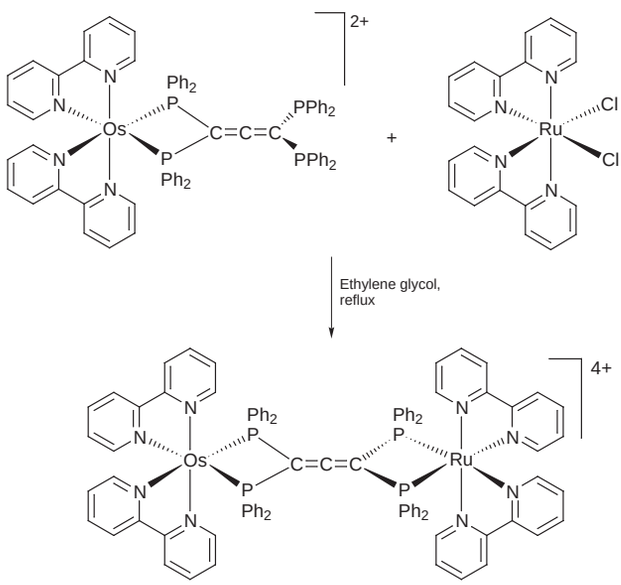


**Scheme 2**

the desired complexes with bis(chelating) phosphines. This is partly due to the fact that a four-membered chelate ring is formed. Another reason is the extremely different solubility of the metal-based precursors and phosphines; while $[M(bpy)_2Cl_2]$ (M = Ru or Os, bpy = 2,2′-bipyridine) is soluble in ethylene glycol, all ligands are intractable in this solvent. Hence, THF is used to introduce ligands into various reaction mixtures, but the refluxing temperature is significantly lower.

In the preparation of monometallic complexes **1a**, **1b**, **2a** or **2b**, a higher ligand-to-metal ratio (2.2–3 : 1) is used. In all cases, the desired complexes are obtained as the dominant products mixed with minor amounts of monosubstituted complexes $[M(bpy)_2Cl(L)]PF_6$ (L = bppe or tppa; M = Ru or Os) and/or bimetallic complexes, Scheme 1. Chromatographic methods have been successfully applied in the separation of the major products. It is found that the combination of basic alumina and acetonitrile or acetonitrile–toluene mixtures provides satisfactory separations and affords products with suitable purities for further analysis.

The homobimetallic complexes **2c**–**2d** are obtained using a suitable metal-to-ligand ratio of typically 2.2 : 1. The heterobimetallic complex **2e** is prepared by the reaction between **2b** and an excess amount of $[Ru(bpy)_2Cl_2]$, Scheme 2. All complexes have been purified using chromatographic separations.

## FAB-MS analysis

Several interesting features are observed in the FAB-MS study of complexes with bppe and tppa. First, it has been found that FAB-MS is a relatively soft ionization technique for these metal complexes. Many of the fragment ions observed only involved sequential loss of counter anions ($PF_6^-$) and $PPh_2$ units, Table 1. Similar observations have been reported in the FAB-MS analysis of ruthenium and osmium complexes with 2,3,5,6-tetrabis(2-pyridyl)pyrazine (TPPZ).[11a] The inner sphere metal–ligand co-ordination was left intact, making peak identification straightforward. Second, the FAB mass spectra of metal–polyphosphine complexes contain numerous informative peaks in which the observed isotope distributions are the same as the simulated ones. Fig. 1(a) shows the representative observed and simulated isotope patterns of $\{[Os(bpy)_2(bppe)]PF_6\}^+$ (*m*/*z* 1045).

In addition to the above features, it is also found that although all metal complexes with polyphosphines are very stable in air (no additional peaks corresponding to the oxidized $PPh_2$ units are observed in the $^{31}P$ NMR spectra of these complexes), oxidation of the $PPh_2$ unit to $OPPh_2$ in phosphines and their metal complexes are observed during the FAB-MS analysis, Fig. 1(b) and 1(c). This is supported by the control experiment using both EI-MS and FAB-MS analysis of polyphosphines. As shown in Fig. 1(c), the FAB-MS spectrum of the ligand tppa gives a complicated spectrum with peaks corresponding to tppa itself ($M^+$, *m*/*z* 777) and the oxidized ligands ($M^+$ + O 793, $M^+$ + 2O 809, $M^+$ + 3O 825), while the EI-MS analysis of the same sample gives a clean spectrum without any peaks corresponding to $OPPh_2$ units [inset in Fig. 1(c)].

## Electrochemical analysis

Cyclic voltammetry has been used to obtain the redox potentials of all complexes synthesized, and the results are given in Table 2. In this section, the redox properties of metal-based oxidations in **1a**, **1b** and **2a**–**2e** will be discussed, followed by the study of ligand-based reductions in these complexes.

The cyclic voltammogram of each of the complexes $[M(bpy)_2(bppe)][PF_6]_2$ (M = Ru **1a** or Os **1b**) is characteristic of a reversible metal-based one-electron process, where reversibility, as used here, implies that the $i_p^a : i_p^c$ ratio is found to be approximately unity.[1,8,10] The $Os^{II}$–$Os^{III}$ redox couple in **1b** is found to be more positive, +1.37 V (*vs.* SCE), when compared with that observed in $[Os(bpy)_3]^{2+}$ (+0.81 V *vs.* SCE) and $[Os(bpy)_2(dppm)]^{2+}$ (+1.27 V *vs.* SCE, dppm = $Me_2PCH_2CH_2PMe_2$).[8b,10] Similarly, the $Ru^{II}$–$Ru^{III}$ redox couple in **1a** is also shifted to +1.70 V, an increase of 0.41 V when compared with +1.29 V in

**Table 1** The FAB-MS analysis of ruthenium and osmium complexes of bppe and tppa

| | Complex | *m*/*z* | Relative abundance (%) | Assignment |
|---|---|---|---|---|
| **1a** | $[Ru(bpy)_2(bppe)][PF_6]_2$ | 955 | 100 | $\{[Ru(bpy)_2(bppe)]PF_6\}^+$ |
| | | 809 | 11 | $[Ru(bpy)_2(bppe)]^+$ |
| **1b** | $[Os(bpy)_2(bppe)][PF_6]_2$ | 1045 | 100 | $\{[Os(bpy)_2(bppe)]PF_6\}^+$ |
| | | 900 | 50 | $[Os(bpy)_2(bppe)]^+$ |
| **2a** | $[Ru(bpy)_2(tppa)][PF_6]_2$ | 1167 | 22 | $\{[Ru(bpy)_2(tppa)]PF_6\}^+ - PPh_2 + O$ |
| | | 1151 | 17 | $\{[Ru(bpy)_2(tppa)]PF_6\}^+ - PPh_2$ |
| | | 1037 | 13 | $[Ru(bpy)_2(tppa)]^+ - PPh_2 + 2O$ |
| | | 1021 | 100 | $[Ru(bpy)_2(tppa)]^+ - PPh_2 + O$ |
| | | 1005 | 27 | $[Ru(bpy)_2(tppa)]^+ - PPh_2$ |
| | | 820 | 7 | $[Ru(bpy)_2(tppa)]^+ - 2PPh_2$ |
| **2b** | $[Os(bpy)_2(tppa)][PF_6]_2$ | 1441 | 9 | $\{[Os(bpy)_2(tppa)]PF_6\}^+ + O$ |
| | | 1425 | 44 | $\{[Os(bpy)_2(tppa)]PF_6\}^+$ |
| | | 1280 | 26 | $[Os(bpy)_2(tppa)]^+$ |
| | | 1273 | 26 | $\{[Os(bpy)_2(tppa)]PF_6\}^+ - PPh_2 + 2O$ |
| | | 1257 | 39 | $\{[Os(bpy)_2(tppa)]PF_6\}^+ - PPh_2 + O$ |
| | | 1241 | 81 | $\{[Os(bpy)_2(tppa)]PF_6\}^+ - PPh_2$ |
| | | 1127 | 25 | $[Os(bpy)_2(tppa)]^+ - PPh_2 + 2O$ |
| | | 1111 | 40 | $[Os(bpy)_2(tppa)]^+ - PPh_2 + O$ |
| | | 1095 | 100 | $[Os(bpy)_2(tppa)]^+ - PPh_2$ |
| | | 911 | 40 | $[Os(bpy)_2(tppa)]^+ - 2PPh_2$ |
| **2c** | $[Ru(bpy)_2(\mu\text{-tppa})Ru(bpy)_2][PF_6]_4$ | 1765 | 100 | $\{[Ru(bpy)_2(tppa)Ru(bpy)_2]PF_6\}^+ + O$ |
| | | 1620 | 17 | $[Ru(bpy)_2(tppa)Ru(bpy)_2]^+ + O$ |
| | | 1435 | 10 | $[Ru(bpy)_2(tppa)Ru(bpy)_2]^+ - PPh_2 + O$ |
| | | 1417 | 15 | $[Ru(bpy)_2(tppa)Ru(bpy)_2]^+ - PPh_2$ |
| **2d** | $[Os(bpy)_2(\mu\text{-tppa})Os(bpy)_2][PF_6]_4$ | 2088 | 6 | $\{[Os(bpy)_2(tppa)Os(bpy)_2][PF_6]_2\}^+ + O$ |
| | | 1943 | 100 | $\{[Os(bpy)_2(tppa)Os(bpy)_2]PF_6\}^+ + O$ |
| | | 1797 | 39 | $[Os(bpy)_2(tppa)Os(bpy)_2]^+ + O$ |
| | | 1280 | 67 | $[Os(bpy)_2(tppa)]^+$ |
| | | 1273 | 67 | $\{[Os(bpy)_2(tppa)]PF_6\}^+ - PPh_2 + 2O$ |
| | | 1257 | 50 | $\{[Os(bpy)_2(tppa)]PF_6\}^+ - PPh_2 + O$ |
| | | 1241 | 17 | $\{[Os(bpy)_2(tppa)]PF_6\}^+ - PPh_2$ |
| | | 1145 | 18 | $[Os(bpy)_2(tppa)]^+ - PPh_2 + 3O$ |
| | | 1127 | 28 | $[Os(bpy)_2(tppa)]^+ - PPh_2 + 2O$ |
| | | 1111 | 41 | $[Os(bpy)_2(tppa)]^+ - PPh_2 + O$ |
| | | 1095 | 25 | $[Os(bpy)_2(tppa)]^+ - PPh_2$ |
| **2e** | $[Os(bpy)_2(\mu\text{-tppa})Ru(bpy)_2][PF_6]_4$ | 1817 | 19 | $\{[Os(bpy)_2(tppa)Ru(bpy)_2][PF_6]_2\}^+ + F$ |
| | | 1798 | 7 | $\{[Os(bpy)_2(tppa)Ru(bpy)_2][PF_6]_2\}^+$ |
| | | 1776 | 18 | $\{[Os(bpy)_2(tppa)Ru(bpy)_2][PF_6]_2\}^+ - F$ |
| | | 1709 | 28 | $[Os(bpy)_2(tppa)Ru(bpy)_2]^+ + O$ |
| | | 1653 | 100 | $\{[Os(bpy)_2(tppa)Ru(bpy)_2]PF_6\}^+ - PPh_2$ |
| | | 1508 | 85 | $[Os(bpy)_2(tppa)Ru(bpy)_2]^+ - PPh_2$ |

**Table 2** Formal potentials (*vs.* SCE) for Ru and Os complexes with bppe and tppa

| | *E*/V *vs.* SCE [relative current intensity] (peak separation, $\Delta E_p$/mV) | | | | |
|---|---|---|---|---|---|
| Complex | $Ru^{II/III}$ | $Os^{II/III}$ | $tppa^{0/-}$ | First $bpy^{0/-}$ | $\Delta E_2^1$* |
| **1a** | +1.70 [1] (80) | | | −1.24 [1] (60) | 2.94 |
| **1b** | | +1.37 [1] (70) | | −1.21 [1] (64) | 2.58 |
| **2a** | +1.55 [1] (70) | | −1.09 [1] (72) | −1.39 [1] (62) | 2.64 |
| **2b** | | +1.12 [1] (74) | −1.10 [1] (60) | −1.32 [1] (82) | 2.20 |
| **2c** | +1.07 [2] (96) | | −1.05 [1] (66) | −1.35 [2] (94) | 2.12 |
| **2d** | | +0.77 [2] (100) | −1.01 [1] (64) | −1.33 [2] (86) | 1.72 |
| **2e** | +1.63 [1] (73) | +0.98 [1] (82) | −1.14 [1] (72) | −1.45 [2] (123) | 2.12 |

* $\Delta E_2^1 = E_2^1(M^{II/III}) - E_2^1$ (first ligand reduction), M = Ru or Os. In compound **2e**, the first metal oxidation is used in the calculation.

$[Ru(bpy)_3][PF_6]_2$.[2,3] This indicates that the species with one chelate bppe ligand are much harder to oxidize. Presumably, this shift is due to the change from more electron donating bpy to the bppe ligand with one double bond. Hence, the $M^{II}$ centers in $[M(bpy)_3]^{2+}$ are more electron rich.

For each of the monometallic complexes with tppa, $[M(bpy)_2(tppa)][PF_6]_2$ (M = Ru **2a** or Os **2b**), a characteristic single metal-based one-electron redox wave is observed. The $Ru^{II}$–$Ru^{III}$ (+1.55 V *vs.* SCE) and $Os^{II}$–$Os^{III}$ (+1.12 V *vs.* SCE) redox potentials are found to significantly shift towards less positive potentials when compared with **1a** and **1b**, correspondingly.

Each of the homobimetallic complexes $[M(bpy)_2(\mu\text{-tppa})M(bpy)_2][PF_6]_4$ (M = Ru **2c** or Os **2d**) features two overlapping one-electron processes, corresponding to two $Ru^{II}$ centers at +1.07 V and two $Os^{II}$ centers at +0.77 V (*vs.* SCE), respectively (Fig. 2). No second metal-based oxidation is observed in the scanned region −1.6 V to +2.0 V. This indicates that the redox interaction between the two metal centers is rather weak, giving simultaneous one-electron oxidation of two metal centers.[11c] Presumably this is due to the orthogonality of the two allenic double bonds, which places the two co-ordination planes of the diphosphine chelates at 90° relative to each other. Here, an additional shift of 0.35–0.48 V towards the less positive potential is observed when compared with the corresponding monometallic complexes **2a** and **2b**. This shift may be due, partially, to the fact that two metal centers are now attached to the central tppa and, as a result, back bonding from each metal center to the polyphosphine tppa is reduced.

The heterobimetallic complex $[Os(bpy)_2(\mu\text{-tppa})Ru(bpy)_2][PF_6]_4$ **2e** features two one-electron processes at +1.63 and

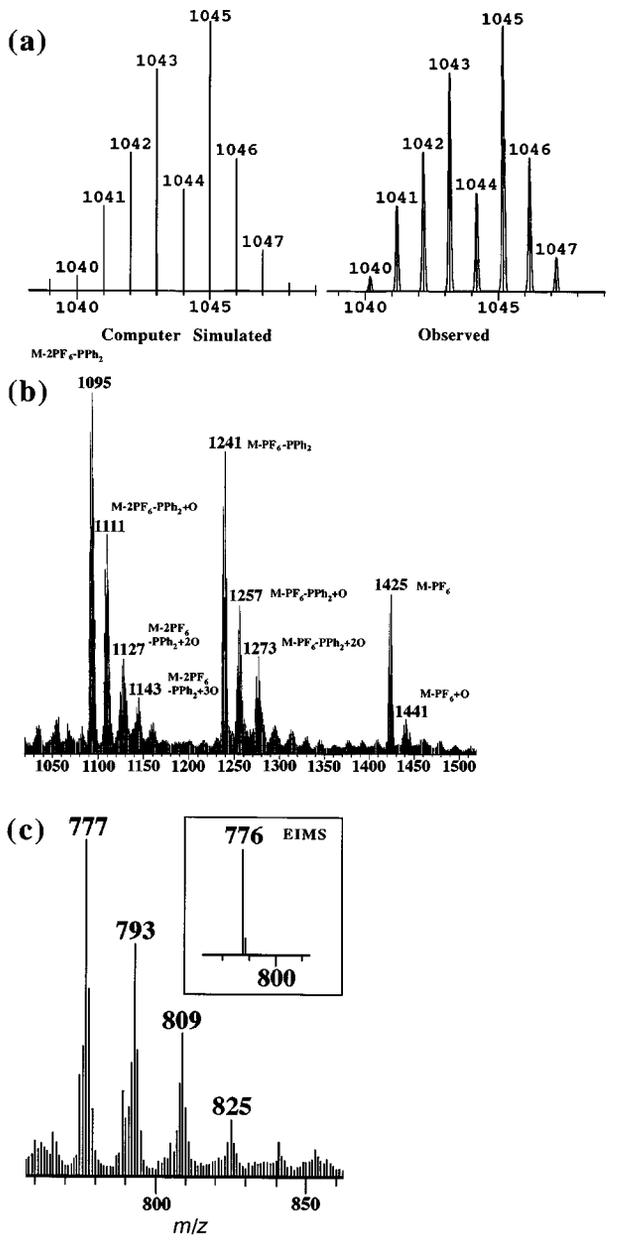


**Fig. 1** (a) Computer simulated and observed isotope patterns of the FAB-MS peak of $\{[Os(bpy)_2(bppe)]PF_6\}^+$ (*m*/*z* 1045). (b) Comparison of the EI-MS (inset) and FAB-MS analysis of the tppa ligand. (c) The FAB-MS analysis of **2b** $\{M = [Os(bpy)_2(tppa)][PF_6]_2\}$

+0.98 V (*vs.* SCE). These two peaks are assigned to $Ru^{II}$–$Ru^{III}$ and $Os^{II}$–$Os^{III}$ redox couples, correspondingly, based on the observed redox potentials in monometallic complexes **2a** and **2b**. Upon scanning anodically, the osmium(II) center is first oxidized at +0.98 V followed by the oxidation of the ruthenium(II) center at +1.63 V, equation (1).

$$Ru^{II}(tppa)Os^{II} \overset{e^-}{\rightleftharpoons} Ru^{II}(tppa)Os^{III} \overset{e^-}{\rightleftharpoons} Ru^{III}(tppa)Os^{III} \quad (2)$$

Several characteristic features are observed for the ligand reduction waves of **1a**, **1b** and **2a**–**2e**. First, both monometallic complexes **1a** and **1b** exhibit consecutive one-electron reduction peaks, with the first peak at −1.24 V and −1.21 V for **1a** and **1b**, respectively (Table 2). Previously, the reported redox potential of the $bpy^{0/-}$ couple was in the range of −1.27 V to −1.31 V for monometallic and bimetallic $Os^{II}$ complexes with 1,2,4,5-tetrakis(diphenylphosphino)benzene.[10] In the electrochemical study of the $[Os(bpy)_2(PPh_2CH{=}CHPPh_2)]^{2+}$ complex, the first

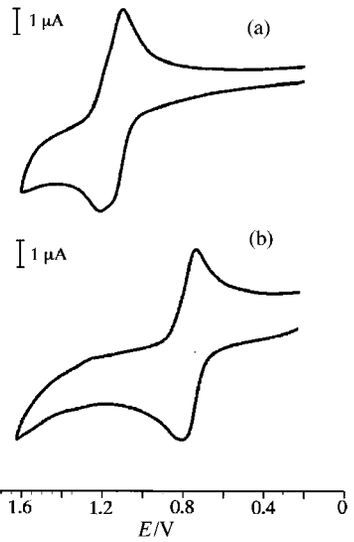


**Fig. 2** Cyclic voltammograms of $[(bpy)_2M(tppa)M(bpy)_2][PF_6]_4$ (M = Ru, a; Os, b): in MeCN, 0.1 mol $dm^{-3}$ $Bu_4NPF_6$, Pt disc working electrode, Pt wire counter electrode, Ag–AgCl reference electrode, scan rate 100 mV $s^{-1}$

ligand reduction peak at −1.26 V (*vs.* SCE) was also assigned to $bpy^{0/-}$.[8c] Hence, the first ligand reduction peaks in **1a** and **1b** are assigned to the $bpy^{0/-}$ couple. The remaining second ligand reduction (−1.50 V in **1a** and −1.43 V in **1b**) corresponds to the second $bpy^{0/-}$ redox couple.[9b] No additional redox wave corresponding to $bppe^{0/-}$ is observed in the scanned range from −2.0 to +2.0 V.

Second, all of the first ligand reduction peaks of the complexes with tppa (**2a**–**2e**) are shifted towards the positive potentials when compared with those observed in complexes with bppe, Table 2. These redox potentials are much more positive than those found for the $bpy^{0/-}$ couple.[8c,10] It is possible that the allene-bridged tppa spacer is reduced before reduction of the auxiliary bpy ligands, and the first one-electron ligand reduction in **2a**–**2e** is assigned to the $tppa^{0/-}$ redox couple. The second ligand reduction is assigned to the first $bpy^{0/-}$ redox wave, Table 2. A similar observation has been reported for the bimetallic complex [Ru(tpy)(L)Os(tpy)] [tpy = 2,2′ : 6′,2″-terpyridine, L = 1,4-bis(2,2′ : 6′,2″-terpyridin-4′-yl)buta-1,3-diyne].[11b] The buta-1,3-diynyl carbon chain bridge is reduced at −1.04 V *vs.* SCE before reduction of the auxiliary tpy ligand at −1.34 V.

Third, the observed peak current of the first ligand reduction (assigned to $tppa^{0/-}$) is about half of the peak current of the second ligand reduction wave (assigned to the first $bpy^{0/-}$ of each metal center) in the bimetallic complexes **2c**–**2e**. This is consistent with a one-electron reduction of the $tppa^{0/-}$ couple in the former and the two overlapping one-electron $bpy^{0/-}$ reductions in the latter (one bpy per metal center). For monometallic complexes **1a**, **1b**, **2a** and **2b**, the observed relative peak currents of the ligand based reductions are approximately equivalent in each complex, corresponding to the one-electron reductions of $tppa^{0/-}$ and $bpy^{0/-}$ couples.

### Electronic absorption spectra

The absorption maxima and the corresponding absorption coefficients of complexes **1a**, **1b** and **2a**–**2e** are listed in Table 3 and their visible region spectra are compared in Fig. 3. The Ru monometallic complex **1a** with bppe exhibits the lowest MLCT (Ru ⟶ bpy) bands at 380 nm (predominantly triplet in character[8a,10]) and the corresponding Os complex **1b** exhibits the lowest MLCT (Os ⟶ bpy) bands at 500 nm (triplet). When compared with the observed values of MLCT bands for $[M(bpy)_3][PF_6]_2$ ($\lambda_{max}$ = 452 nm for M = Ru,[12] and 640 nm for M = Os[8b]), the corresponding MLCT bands in **1a** and **1b** are

**Table 3** Summary of spectroscopic data

| Complex | $\lambda_{abs}$/nm ($\varepsilon$/dm$^3$ mol$^{-1}$ cm$^{-1}$) | $\lambda_{em}$[a]/nm | $10^{-3}\Phi$ (±10%)[a,b] | $\tau$[a]/ns (±10%) Ru-based | Os-based | $\eta_{isc}k_r$[c]/s$^{-1}$ |
|---|---|---|---|---|---|---|
| **1a** | 280 (39 840), 380 (11 300) | 530 | 0.40 | 25 | | $1.6 \times 10^4$ |
| **1b** | 280 (32 600), 385 (8960), 500 (2840) | 600 | 30 | | 190 | $1.6 \times 10^5$ |
| **2a** | 290 (40 700), 400 (9810), 450 (sh) (6040) | 535 | 0.11 | 40 | | $2.8 \times 10^3$ |
| **2b** | 290 (44 050), 360 (13 050), 450 (8100), 550 (sh) (2800) | 570 | 2.3 | | 350 | $6.6 \times 10^3$ |
| **2c** | 290 (57 200), 320 (17 900), 450 (7950) | 560 | 0.16 | 45 | | $3.6 \times 10^3$ |
| **2d** | 295 (47 900), 370 (8950), 460 (6700), 605 (2050) | 580 | 1.9 | | 520 | $3.7 \times 10^3$ |
| **2e** | 290 (71 200), 420 (13 200), 550 (sh) (3100) | 590 | 7.0 | 0.33[d]<br>5.9[d] | 410[d] | $1.7 \times 10^4$ |

[a] $\lambda_{ex} = 470$ nm, in acetonitrile. All solution samples were treated with three freeze–pump–thaw cycles before the measurements of emission and quantum yields. Luminescence lifetimes are obtained from the least-squares fit of single or double exponential decay. [b] $\Phi_{em}$ *vs.* $[Ru(bpy)_3][PF_6]_2$ ($\Phi_{em} = 0.062$). [c] $\eta_{isc}k_r = \Phi_{em}\tau^{-1}$. In **2e**, $\tau_2$ is used in the calculation. [d] The short component in the lifetime of **2e** was measured on a frequency domain fluorimeter (measurable range 50 ps–50 ns, excitation at 470 nm, monitored broadband with a cut-off filter at 500 nm). The long component in the lifetime of **2e** is obtained (as is the rest of the data in this table) on a nanosecond laser system equipped with a Continuum Surelite II-10 Nd : YAG laser (lowest measurable lifetime is *ca.* 10 ns with a 6 ns laser pulse width; excitation at 470 nm, monitoring emission wavelength at 590 nm).

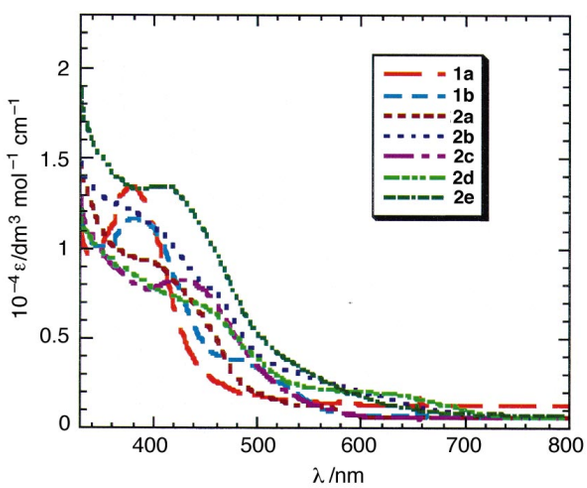


**Fig. 3** Comparison of the electronic absorption spectra of **1a**, **1b** and **2a**–**2e**

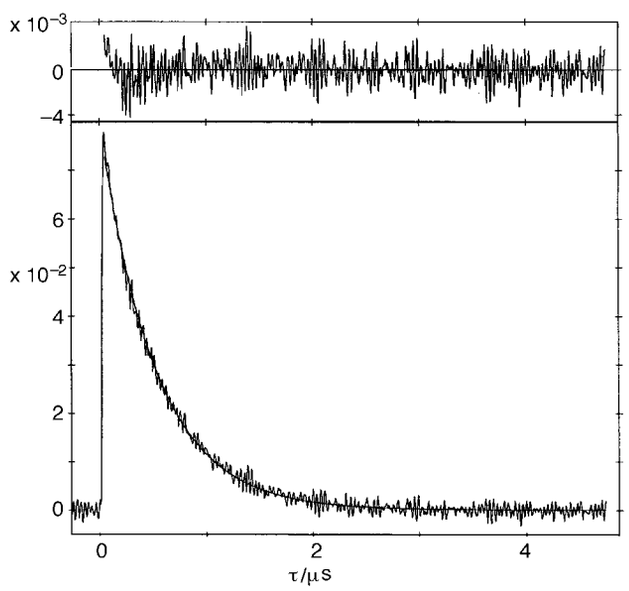


**Fig. 4** Excited state decay trace and fit of **2d**: $\lambda_{ex} = 470$, $\lambda_{em} = 590$ nm, in spectrograde acetonitrile at 295 K (freeze–pump–thaw three times prior to use)

significantly blue-shifted. Similar blue-shift of the MLCT band has also been reported in the previous study of $[Os(bpy)_2(L)_2]^{2+}$ (L = phosphines such as $PPh_3$, $PMe_2Ph$, dppm, *etc.*) complexes.[8b,10,13a] This blue-shift is ascribed to the stabilization of the ground state by the enhanced dπ(M)–dπ(L) back bonding and the destabilization of the excited state by the poorer σ-donating phosphine ligand.[10,13a]

The $^3$MLCT (M ⟶ bpy) bands of complexes **2a** and **2b** bearing tppa are broad with $\lambda_{max}$ at approximately 450 nm for **2a** and 550 nm for **2b**, all of which are red-shifted from the observed values of **1a** and **1b**. The homobimetallic complexes **2c** and **2d** exhibit charge-transfer bands with $\lambda_{max} = 450$ and 460 nm, respectively. An additional weak absorption band at 605 nm was also observed in **2d**, Fig. 3. These values are further red-shifted from the corresponding monometallic complex **2a** and **2b**. In the heterobimetallic complex **2e** a broad absorption band with $\lambda_{max}$ at *ca.* 420 nm is observed, with a shoulder peak tailing into 550 nm.

### Emission and excited state lifetimes

Steady-state and time-resolved emission spectroscopy have been used to study the excited-state properties, including room-temperature luminescence, quantum yields and luminescence lifetimes. All data are summarized in Table 3.

When compared with the luminescence properties of $[M(bpy)_3][PF_6]_2$ (M = Ru, $\lambda_{em} = 620$ nm;[14a] M = Os, $\lambda_{em} = 723$ nm[12a]), blue-shifted emission maxima (shift of about 60–95 nm in Ru complexes **1a**, **2a** and **2c**, and of about 120–150 nm for Os complexes **1b**, **2b** and **2d**) have been observed in all mono- and homobi-metallic complexes with bppe and tppa ligands. This indicates that the replacement of one bpy ligand by either bppe or tppa increases the energy gap between the ground state and the $^3$MLCT excited state. Such a blue-shift in emission is expected when a stronger ligand (such as a polyphosphine) is used to replace a relatively weak ligand (such as bpy).[8]

Time-resolved emission studies of complexes **1a**, **1b** and **2a**–**2e** have also been carried out at room temperature. The emission decay traces of all complexes, except **2e**, fit to single-exponential decay curves, giving excited-state lifetimes as listed in Table 3. A representative decay trace and fit for **2d** are shown in Fig. 4. The lifetimes of all $Os^{II}$ complexes are much longer than that of $[Os(bpy)_3][PF_6]_2$ ($\tau = 20$ ns in acetonitrile[10,12b]). Such a change in lifetime can be ascribed to the increased energy gap between the ground state and the emitting $^3$MLCT state, according to the energy gap law.[8–10] Although phosphines do not absorb light, they will cause an increase of the $^3$MLCT excited states and, consequently, slow the non-radiative decay of $Os^{II}$ complexes and result in longer excited-state lifetimes. In contrast to $Os^{II}$ complexes, $Ru^{II}$ compounds with bppe and tppa have much shorter lifetimes when compared with $[Ru(bpy)_3][PF_6]_2$ ($\tau = 855$ ns in acetonitrile[14a]), presumably due to the mixing of the lowest dπ(M)–π*(L) charge transfer band with higher energy excited states.[10,12] While blue-shifted emis-

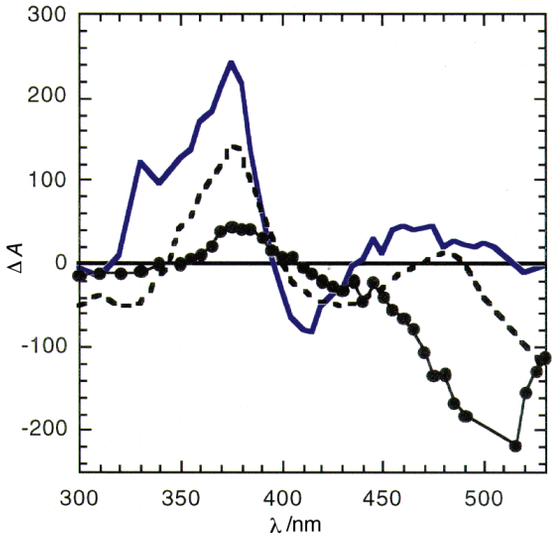


**Fig. 5** Differential absorption spectra of **1b** (——, $\lambda_{ex} = 520$), **2b** (– – –, $\lambda_{ex} = 520$) and **2d** (•–•–•, $\lambda_{ex} = 510$ nm) in deoxygenated spectrograde MeCN at 25 °C

sions are also observed in complexes **1a** and **2a** when compared with $[Ru(bpy)_3][PF_6]_2$, the changes in their excited state lifetimes cannot be attributed solely to the energy gap law.

The radiative decay rate constant, $k_r$, can also be calculated from the emission quantum yield and the lifetime of emitting MLCT state ($k_r = \Phi_{em}/\tau$). This calculation is only correct if the efficiency of population of the emitting $^3$MLCT state is unity,[14] since the observed radiative decay rate constant includes the intersystem crossing efficiency, $\eta_{isc}$, to populate the $^3$MLCT states. When $\eta_{isc}$ is included, $k_r$ can be expressed as $k_r = \Phi_{em}/\eta_{isc}\tau$ or $\eta_{isc}k_r = \Phi_{em}/\tau$. All calculated data of $\eta_{isc}k_r$ are listed in Table 3. These $\eta_{isc}k_r$ values are found to be sensitive to the phosphines involved. Relatively high values of $\eta_{isc}k_r$ are found in complexes **1a** and **1b** with bppe ($1.6 \times 10^4$ and $1.6 \times 10^5$ $s^{-1}$ respectively) when compared with much lower values in complexes **2a**–**2e** with tppa (Table 3, with the lowest value at $2.8 \times 10^3$ $s^{-1}$). These low observed radiative decay constants may imply either rapid relaxation of the $^1$MLCT state back to the ground state or formation of another state.[4c] Ruthenium(II) diimine complexes have been found to have an efficient intersystem crossing from the $^1$MLCT state to the $^3$MLCT state.[4c,13b,c] However, we cannot presently exclude or address the possibility of a diminished intersystem crossing efficiency in complexes with the tppa ligand. A similar observation has been reported by Schmehl and co-workers[4c] in the study of mono- and bimetallic ruthenium(II) diimine complexes. Among a series of complexes, the lowest $\eta_{isc}k_r$ value of 6700 $s^{-1}$ was reported for the complex $[Ru(dmb)_2(bbdb)]^{2+}$ while a higher $\eta_{isc}k_r$ value of $1.1 \times 10^5$ $s^{-1}$ was obtained for $[Ru(dmb)_3]^{2+}$ [dmb = 4,4′-dimethyl-2,2′-bipyridine; bbdb = 1,4-bis(4′-methyl-2,2′-bipyridin-4-yl)buta-1,3-diene].

Upon excitation at 510–520 nm, the differential absorption spectra of $Os^{II}$ complexes with bppe and tppa are obtained and compared in Fig. 5. All spectra have a characteristic absorption peak around 375 nm (corresponding to the absorbing $\pi \longrightarrow \pi^*$ of co-ordinated bipyridine) and bleaching of the MLCT absorption band in the region of 410–550 nm. Additional weak transient absorption bands are observed for **1b** and **2b** around 420–460 nm, which can be ascribed to the weakly absorbing charge-transfer bands. Several attempts have been made to detect the transient absorption signals of other systems with $Ru^{II}$ centers but have failed to provide any observable signal.

**Energy transfer.** In the heterobimetallic complex **2e**, excitation in acetonitrile at 550 nm, where the $Os^{II}$ component is the dominant chromopore, results in the appearance of the luminescence centered around 590 nm, characteristic of the emission from the $Os^{II}$-based chromophore. Upon excitation at 470 nm (where the $Ru^{II}$-based chromophore absorbs approximately 50% of the incident photons), only emission at 590 nm is observed, also characteristic of the $Os^{II}$ component. Furthermore, the corrected luminescence excitation spectrum of **2e**, when monitoring at the $Os^{II}$ emission wavelength of 590 nm, was found to have a close match with the corresponding absorption spectrum in the visible region of 400 to 570 nm. All the above results suggest the presence of energy transfer. Because of the well known energy difference between the lowest energy excited states of $Ru^{II}$ and $Os^{II}$ polypyridine complexes, electronic energy transfer is expected to occur from the Ru-based unit to the Os-based one.[2,6,15–19] Following the conventional assumptions,[15–19] the free energy change $\Delta G^0$ can be expressed as the difference between the spectroscopic energies of the energy donor (Ru-based) and acceptor (Os-based). The actual calculated value is *ca.* 1150 $cm^{-1}$ or 0.14 eV between Ru- and Os-based units, estimated from the energy of the emission maxima of monometallic complexes with the tppa ligand.

The energy transfer rate constant $k_{en}$ can be estimated by equation (2)[17] where $\tau_m$ and $\tau$ represent the luminescence lifetimes of the model complex and the system in question. By exciting the MLCT band at 470 nm, a single exponential decay is observed for the $^3$MLCT excited state of the model compound **2a**, and the lifetime is found to be $\tau_m = 40$ ns. For the heterobimetallic complex **2e**, a long lifetime component of 410 ns is observed when measured using our nanosecond laser system (see Experimental section). This lifetime is comparable to that of the corresponding monomeric compound **2b** within the range of experimental error, indicating an emission from the $Os^{II}$ part of **2e**. In order to probe the lifetime of the quenched $Ru^{II}$ excited state, measurement on a frequency domain fluorimeter was carried out (measurable range 50 ps–50 ns). Two additional short-lived components were revealed with $\tau_1 = 0.33$ and $\tau_2 = 5.9$ ns. Both components are much shorter than the $^3$MLCT lifetimes observed in **2a** or **2c**. Although it is expected to observe a quenched shorter lifetime from the $Ru^{II}$ part of **2e** as the result of intramolecular energy transfer from the Ru-based unit to the $Os^{II}$-based one, we are not clear about the other possible quenching mechanism that may cause the presence of two short components in the lifetime of **2e**. From these two short components of lifetime, the rate constant of energy transfer in **2e** can be estimated, using equation (2), to be higher than $1.4 \times 10^8$ but not exceeding $3.0 \times 10^9$ $s^{-1}$, assuming energy transfer is responsible for the decrease of the $Ru^{II}$ excited-state lifetime.

$$k_{en} = 1/\tau - 1/\tau_m \qquad (2)$$

**Mechanism of intramolecular energy transfer.** In order to study the mechanism by which intramolecular energy transfer occurs in complex **2e** with a tppa spacer, the spectroscopic overlap integral and the energy transfer rate constant are calculated here.[11b–d,17] Previously, the energy transfer processes that take place in systems similar to **2e**, but involve other types of flexible[18,20] (*e.g.* alkanes) or rigid spacers[11,12b,c,17] (*e.g.* polyphenylene), have been interpreted as occurring *via* a Föster- and/or Dexter-type mechanism.

For energy transfer *via* a Föster-type dipole–dipole (*i.e.* through space) mechanism, the appropriate spectroscopic overlap integral ($J_F$) can be expressed as equation (3).[11b,c,21] Here

$$J_F = \frac{\int F(\nu)\varepsilon(\nu)\nu^{-4}d\nu}{\int F(\nu)d\nu} \qquad (3)$$

$F(\nu)$ is the luminescence intensity at wavelength $\nu$ (in $cm^{-1}$), and $\varepsilon(\nu)$ is the molar absorption coefficient (in $dm^3$ $mol^{-1}$ $cm^{-1}$).[11b]

The $J_F$ value thus calculated is $1.1 \times 10^{-13}$ cm$^6$ mol$^{-1}$ (±10%) for the heterobimetallic complex **2e**. The derived value here is of comparable magnitude to the estimated overlap integrals previously reported for systems with rigid alkyne-[11d] or phenylene-bridged[17] Ru/Os complexes. The rate constant for triplet energy transfer occurring by the Föster mechanism can then be calculated using equation (4)[11b,c] where $K$ is the orientation factor

$$k_F = \frac{8.8 \times 10^{-25} K^2 \Phi_L J_F}{n^4 \tau_L R^6} \quad (4)$$

relating to the alignment of transition dipoles on donor and acceptor ($K^2 = 0.67$[11d]), $\Phi_L$ and $\tau_L$ are the quantum yield and excited-state lifetime of the appropriate monomeric complex **2a**, and $n$ is the refractive index of the solvent acetonitrile. At 295 K the calculated $k_F$ value is $(9 \pm 1) \times 10^7$ s$^{-1}$ for an Ru–Os distance of *ca.* 9 Å.[22] This calculated Föster energy-transfer rate constant is lower than the observed energy-transfer rate constant for **2e**.

The Dexter-type energy transfer can be described as a double exchange of electrons (*i.e. via* direct or superexchange-mediated electronic interaction) between donor and acceptor.[1,11d,17,23] The rate constant of such an energy transfer can be expressed in the non-adiabatic limit as in equation (5). The electronic frequency

$$k_{en} = \nu_{en} \exp[-\Delta G^{\ddagger}/RT] \quad (5)$$

$\nu_{en}$ and the free activation energy $\Delta G^{\ddagger}$ can be evaluated according to equations (6) and (7).[1,17] Here $\Delta G^0$ is the difference

$$\nu_{en} = (2H_{en}^2/h)(\pi^3/\lambda RT)^{\frac{1}{2}} \quad (6)$$

$$\Delta G^{\ddagger} = (\lambda/4)(\lambda + \Delta G^0/\lambda)^2 \quad (7)$$

between the spectroscopic energies of donor and acceptor (*ca.* 1150 cm$^{-1}$ or 0.14 eV). The reorganization energy λ can be estimated from the Stokes shift[17] of the acceptor (*ca.* 800 cm$^{-1}$ or 0.10 eV). The calculated value of $\exp[-\Delta G^{\ddagger}/RT]$ is approximately 1 and, hence, $k_{en}$ is almost equal to $\nu_{en}$. From equation (6) $\nu_{en}$ is estimated as $(8.2 \times 10^8)H_{en}^2$ cm$^{-2}$. If the energy transfer occurs exclusively *via* an electron exchange mechanism, the calculated $k_{en}$ value would be equal to the observed one ($1.4 \times 10^8$–$3.0 \times 10^9$ s$^{-1}$), and the electronic coupling matrix element $H_{en}$ can then be estimated to be 0.4–2 cm$^{-1}$ by the assumption of an exchange mechanism. Such a small $H_{en}$ value corresponds to a situation in which the Ru and Os centers are almost in electronic isolation.[11b] The aforementioned electrochemical study has shown that the redox interaction across the tppa spacer with an allene bridge is rather weak. Based on all above calculations and observations, we conclude that the Dexter energy-transfer mechanism may be involved in the observed energy-transfer process in the heterobimetallic Ru–Os complex with the tppa spacer.

## Conclusion

We have found that Ru and Os complexes with the polyphosphines bppe and tppa exhibit room-temperature luminescence, with long $^3$MLCT excited-state lifetimes of monometallic and bimetallic Os complexes. The two moieties spanned by the tppa spacer are in electronic isolation, however, the energy transfer across the same bridging ligand is found to be efficient from the Ru-based unit to the Os-based one. We are currently exploring the preparation, electrochemical and spectroscopic properties of the luminescent and redox-active complexes containing polyphosphine spacers with longer cumulenic $C_n$ bridges. Details regarding the effect of various cumulenic $C_n$ bridges on the redox interaction and energy transfer or electron transfer between two metal centers spanned by this type of rigid spacer will be investigated and reported later.

## Experimental

### General procedures

All reactions pertaining to the preparation of metal–polyphosphine complexes were carried out under an $N_2$ atmosphere and in the dark. Column chromatographic separation was performed in the dark using basic alumina (Brockman activity I, 60–325 mesh, from Fisher Scientific) and acetonitrile or toluene–acetonitrile (40 : 60, v/v) as eluent.

### Materials

1,1′,3,3′-Tetrakis(diphenylphosphino)allene (tppa),[24,25] 1,1′-bis(diphenylphosphino)ethene (bppe)[25,26] and *cis*-[Os(bpy)$_2$Cl$_2$][27] were prepared according to the literature methods. The complex *cis*-[Ru(bpy)$_2$Cl$_2$] was purchased from Strem and used as received. Commercial grade solvents (acetonitrile, diethyl ether, toluene, methanol and ethanol) were dried over 4 Å molecular sieves prior to use. Tetrahydrofuran (THF) was dried and deoxygenated by heating to reflux under $N_2$ for at least 24 h over sodium benzophenone ketyl and was freshly distilled prior to use. Commercial grade ethylene glycol was dried over 4 Å molecular sieves for at least 24 h and deoxygenated by degassing with dry $N_2$ for 10 min or longer before it was used in reactions. Basic alumina was purchased from Fisher and directly used in chromatographic separations. All spectrograde solvents were also purchased from Fisher and used without further purification.

### Instrumentation

The $^{31}$P-{$^1$H} NMR spectra were obtained in $CD_3CN$ on an Omega 500 MHz spectrometer. Electron ionization and fast atom bombardment mass spectral analysis (EI-MS and FAB-MS) were recorded on a Fisions VG Autospec at the UCI Mass Spectral Laboratory. Absorbance spectra were recorded on a Hewlett-Packard 8453 diode array spectrophotometer. Steady-state emission spectra were obtained on an Hitachi F-4500 fluorescence spectrometer. Luminescence quantum yields of all complexes were measured in spectrograde acetonitrile relative to [Ru(bpy)$_3$][PF$_6$]$_2$ ($\Phi = 0.062$[14] in acetonitrile). All samples were treated with three freeze–pump–thaw cycles prior to measurements. The time-resolved emission spectroscopic studies were carried out on a nanosecond flash photolysis unit equipped with a Continuum Surelite II-10 Q-switched Nd : YAG laser and Surelite OPO (optical parametric oscillator) tunable visible source, a LeCroy 9350A oscilloscope, and a Spex 270 MIT-2x-FIX high performance scanning and imaging spectrometer.

### Syntheses

**[M(bpy)$_2$(bppe)][PF$_6$]$_2$, M = Ru 1a or Os 1b.** In a 100 mL three-necked flask (Ph$_2$P)$_2$C=CH$_2$ (155 mg, 0.39 mmol) was dissolved in 15 mL of dry THF and heated to reflux under $N_2$. To this solution a 15 mL ethylene glycol solution of 0.13 mmol [M(bpy)$_2$Cl$_2$]·2H$_2$O (M = Ru, 68 mg; M = Os, 75 mg), degassed with dry $N_2$ for at least 10 min prior to use, was added dropwise using a pressure-equalizing funnel. The resulting mixture was refluxed for 2 h. An excess amount of $NH_4PF_6$ (200–300 mg) was added and the mixture was refluxed for up to 60 h to ensure the completion of reaction. The solution was cooled to room temperature, and the THF was removed on a rotary evaporator. The resulting ethylene glycol solution was added dropwise to 100 mL of a saturated aqueous $KPF_6$ solution. The precipitate was collected by vacuum filtration, washed with 20 mL $H_2O$

(2 ×) and 20 mL diethyl ether (3 ×), and vacuum dried overnight. The product thus obtained was chromatographically separated on basic alumina using acetonitrile as eluent to give the desired product as the second fraction. The first fraction, a minor product (5–20%) using toluene–acetonitrile (40 : 60, v/v) as eluent, was found to be $[M(bpy)_2Cl(bppe)]PF_6$. Complex **1a**: Yield 135 mg (95%) (Found: C, 50.05; H, 5.03; N, 4.50. Calc. for $C_{46}H_{38}F_{12}N_4P_4Ru$: C, 50.24; H, 3.48; N, 5.10%). $^{31}P$-{$^1H$} NMR ($CD_3CN$, 202 MHz, 22 °C): δ 18.21. Complex **1b**: Yield 96 mg (63%) (Found: C, 47.41; H, 3.85; N, 5.06. Calc. for $C_{46}H_{38}F_{12}N_4OsP_4$: C, 46.47; H, 3.22; N, 4.71%). $^{31}P$-{$^1H$} NMR ($CD_3CN$, 202 MHz, 22 °C): δ −23.32.

**$[M(bpy)_2(tppa)][PF_6]_2$, M = Ru 2a or Os 2b.** A procedure analogous to that for the preparation of **1a** and **1b** was followed with ligand-to-metal ratios of 2.2–3 : 1 and a refluxing period up to 60 h to ensure the completion of reaction. The product was separated on basic alumina using acetonitrile to give the desired product as the first fraction. A small amount (<20%) of the bimetallic complexes **2c** or **2d** could also be isolated as the second fraction using methanol as eluent. With a short refluxing period, a minor amount of the monosubstituted complex $[M(bpy)_2Cl(tppa)]PF_6$ could also be isolated as the first fraction (the yield of this product varied as the refluxing time was changed) using toluene–acetonitrile (40 : 60, v/v) as eluent, the desired compound was obtained as the second fraction using acetonitrile as eluent. Complex **2a**: Yield 193 mg (80%) from 85 mg $[Ru(bpy)_2Cl_2]\cdot 2H_2O$ and 296 mg tppa (Found: C, 56.00; H, 4.52; N, 4.10. Calc. for $C_{51}H_{56}F_{12}N_4P_4Ru\cdot 2H_2O$: C, 56.25; H, 3.99; N, 3.70%). $^{31}P$-{$^1H$} NMR ($CD_3CN$, 202 MHz, 22 °C): δ 2.34, −30.22. Complex **2b**: Yield 230 mg (89%) from 100 mg $[Os(bpy)_2Cl_2]\cdot 2H_2O$ and 296 mg tppa (Found: C, 52.80; H, 3.94; N, 3.97. Calc. for $C_{51}H_{56}F_{12}N_4OsP_4\cdot 2H_2O$: C, 53.12; H, 3.77; N, 3.49%). $^{31}P$-{$^1H$} NMR ($CD_3CN$, 202 MHz, 22 °C): δ −30.49, −37.37.

**$[M(bpy)_2(\mu\text{-tppa})M(bpy)_2][PF_6]_4$, M = Ru 2c or Os 2d.** These compounds could be obtained as side products in the preparation of **2a** and **2b**. They could also be prepared using the metal-to-ligand ratio of *ca.* 2.2 : 1. In a 100 mL three-necked flask a 15 mL ethylene glycol solution containing 0.164 mmol of $[M(bpy)_2Cl_2]\cdot 2H_2O$ was degassed with dry $N_2$ for at least 10 min and then heated to above 120 °C. To this solution 0.075 mmol of tppa in 30 mL THF was added dropwise *via* a pressure-equalizing funnel. The resulting mixture was refluxed for 2 h. Excess $NH_4PF_6$ was then added and the mixture was refluxed for up to 60 h to ensure the completion of reaction. The solution was cooled to room temperature, and THF was removed on a rotary evaporator. The resulting ethylene glycol solution was added dropwise to 100 mL of saturated aqueous $KPF_6$ solution. The precipitate was collected by vacuum filtration, washed with 20 mL $H_2O$ (2 ×) and 20 mL diethyl ether (3 ×), and vacuum dried overnight. The product was separated on a basic alumina column, using acetonitrile as eluent, to give the desired product as the second fraction. A small amount (10–20%) of the monometallic complexes **2a** or **2b** was obtained as the first fraction, using toluene–acetonitrile (40 : 60, v/v) as eluent. Complex **2c**: Yield 61% (Found: C, 50.69; H, 3.72; N, 5.60. Calc. for $C_{91}H_{72}F_{24}N_8P_8Ru_2$: C, 50.06; H, 3.32; N, 5.13%). $^{31}P$-{$^1H$} NMR ($CD_3CN$, 202 MHz, 22 °C): δ 140.87. Complex **2d**: Yield 155 mg (85%) (Found: C, 46.45; H, 3.55; N, 4.98. Calc. for $C_{71}H_{72}F_{24}N_8Os_2P_8$: C, 46.28; H, 3.07; N, 4.75%). $^{31}P$-{$^1H$} NMR ($CD_3CN$, 202 MHz, 22 °C): δ 83.64.

**$[Ru(bpy)_2(\mu\text{-tppa})Os(bpy)_2][PF_6]_4$ 2e.** In a 100 mL three-necked flask 62 mg, 0.0384 mmol of complex **2b** and 20 mg, 0.0384 mmol of $[Ru(bpy)_2Cl_2]\cdot 2H_2O$ were added together and purged with $N_2$, 20 mL of degassed ethylene glycol was added and the resulting solution was heated at refluxing temperature for 6 h. The solution was then cooled to room temperature, and added dropwise to a 100 mL saturated aqueous solution of $KPF_6$. The brown precipitate thus formed was collected using vacuum filtration, washed with 20 mL water (2 ×) and 20 mL diethyl ether (3 ×), and vacuum dried overnight. The product was separated on basic alumina using acetonitrile as eluent, and the desired product was collected as the second fraction. Yield 65 mg (74%) (Found: C, 46.93; H, 4.47; N, 4.83. Calc. for $C_{71}H_{72}F_{24}N_8OsP_8Ru\cdot 4H_2O$: C, 46.62; H, 3.44; N, 4.78%). $^{31}P$-{$^1H$} NMR ($CD_3CN$, 202 MHz, 22 °C): δ 90.37, −31.14.

### Characterization of complexes by fast atom bombardment mass spectrometry

In addition to elemental analysis and $^{31}P$-{$^1H$} NMR spectral analysis, all the above complexes have also been studied using FAB-MS. 3-Nitrobenzyl alcohol was used as the matrix. A compilation of the peaks of higher mass in the spectrum of each complex, along with their assignment, is presented in Table 1.

### Electrochemical analysis

Cyclic voltammetry measurements were performed in a standard three-electrode cell. A Ag–AgCl wire was used as a pseudo-reference electrode, a platinum wire as the counter-electrode, and a 1.0 mm platinum disk electrode as the working electrode. A solution of the purified electrolyte in acetonitrile (0.1 mol $dm^{-3}$) was first scanned to ensure the absence of air, water and other impurities. Cyclic voltammograms were recorded with a CHI 630 electrochemical analyzer, with a scan rate of 100 mV $s^{-1}$. All experiments were referenced, after all scans had been taken, against an added ferrocene standard. No *i*R compensation was applied.

## Acknowledgements

This work was supported by the UCI Startup Funds, the Faculty Research Grant from UCI Academic Senate Committee on Research, and National Science Foundation CAREER award (CHE-9733546). S. K. S. acknowledges financial support from the Undergraduate Research Opportunity Program at UCI. J. V. O. acknowledges support from the Graduate and Professional Opportunity Program (GPOP) from the US Department of Education. We thank Dr. Torbjoern Pascher from the California Institute of Technology and Dr. Wytze van der Veer at the UCI Laser Facility for their help in the set-up of a nanosecond laser system for the time-resolved emission study. We also thank Professor Wayne E. Jones, Jr. and his graduate student Clifford Murphy for the measurement of short lifetimes of compound **2e**, and Dr. John Greaves at the UCI Mass Spectral Laboratory for his assistance in the FAB-MS analysis.

## References

1 J.-P. Sauvage, J.-P. Colin, J.-C. Chambron, S. Guillercz, C. Cudret, V. Balzani, F. Barigelletti, L. De Cola and L. Flamigni, *Chem. Rev.*, 1994, **94**, 993; V. Balzani, A. Juris, M. Venturi, S. Campagna and S. Serroni, *Chem. Rev.*, 1996, **96**, 759.

2 M. Brady, W. Weng, Y. Zhou, J. W. Seyler, A. J. Amoroso, A. M. Arif, M. Böhme, G. Frenking and J. A. Gladysz, *J. Am. Chem. Soc.*, 1997, **119**, 775; K. Wärnmark, J. A. Thomas, O. Heyke and J.-M. Lehn, *Chem. Commun.*, 1996, 701.

3 T. J. Meyer, *Pure Appl. Chem.*, 1986, **58**, 1193; A. Harriman and R. Ziessel, *Chem. Commun.*, 1996, 1707.

4 (*a*) F. Scandola, R. Argazzi, C. A. Bignozzi, C. Chiorboli, M. T. Indelli and M. A. Rampi, *Coord. Chem. Rev.*, 1993, **125**, 283; (*b*) P. Belser, R. Dux, M. Baak, L. De Cola and V. Balzani, *Angew. Chem., Int. Ed. Engl.*, 1995, **34**, 595; (*c*) A. I. Baba, H. E. Ensley and R. H. Schmehl, *Inorg. Chem.*, 1995, **34**, 1198.

5 B.Hong and J. V. Ortega, *Angew. Chem., Int. Ed. Engl.*, 1998, in the press; B. Hong, *Comments Inorg. Chem.*, 1998, in the press; F. A. Cotton and B. Hong, *Prog. Inorg. Chem.*, 1992, **40**, 179.

6 F. A. Cotton, B. Hong, M. Shang and G. G. Stanley, *Inorg. Chem.*, 1993, **32**, 3620.

7 V. Balzani and F. Scandola, *Supramolecular Photochemistry*, Horwood, Chichester, 1991.
8 (*a*) E. M. Kober, J. V. Caspar, B. P. Sullivan and T. J. Meyer, *Inorg. Chem.*, 1988, **27**, 4587; (*b*) S. R. Johnson, T. D. Westmoreland, J. V. Caspar, K. R. Barqawi and T. J. Meyer, *Inorg. Chem.*, 1988, **27**, 3195; (*c*) E. M. Kober, B. P. Sullivan, W. J. Dressick, J. V. Caspar and T. J. Meyer, *J. Am. Chem. Soc.*, 1980, **102**, 7383; (*d*) J. V. Caspar, E. M. Kober, B. P. Sullivan and T. J. Meyer, *J. Am. Chem. Soc.*, 1982, **104**, 630.
9 (*a*) R. G. Brewer, G. E. Jensen and K. J. Brewer, *Inorg. Chem.*, 1994, **33**, 124; (*b*) M. M. Richter and K. J. Brewer, *Inorg. Chem.*, 1993, **32**, 5762; (*c*) M. M. Richter and K. J. Brewer, *Inorg. Chem.*, 1993, **32**, 2827.
10 P.-W. Wang and M. A. Fox, *Inorg. Chem.*, 1995, **34**, 36.
11 (*a*) C. R. Arana and H. D. Abruna, *Inorg. Chem.*, 1993, **32**, 194; (*b*) V. Grosshenny, A. Harriman, M. Hissler and R. Ziessel, *J. Chem. Soc.*, *Faraday Trans.*, 1996, **92**, 2223; (*c*) V. Grosshenny, A. Harriman, F. M. Romero and R. Ziessel, *J. Phys. Chem.*, 1996, **100**, 17 472; (*d*) V. Grosshenny, A. Harriman, M. Hissler and R. Ziessel, *Angew. Chem.*, *Int. Ed. Engl.*, 1995, **34**, 1100.
12 (*a*) C. Creutz, M. Chou, L. Netzel, M. Okumura and N. Sutin, *J. Am. Chem. Soc.*, 1980, **102**, 1309; (*b*) F. Barigelletti, A. Juris, V. Balzani, P. Belser and A. von Zelewsky, *Inorg. Chem.*, 1983, **22**, 3335; (*c*) A. Juris, P. Belser, F. Barigelletti, A. von Zelewsky and V. Balzani, *Inorg. Chem.*, 1986, **25**, 256; (*d*) J. R. Winkler, T. L. Netzel, C. Creutz and N. Sutin, *J. Am. Chem. Soc.*, 1987, **109**, 2381; (*e*) Y. Fuchs, S. Lofters, T. Dieter, W. Shi, R. Morgan, T. C. Strekas, H. D. Gafney and A. D. Baker, *J. Am. Chem. Soc.*, 1987, **109**, 2691.
13 (*a*) J. V. Caspar, T. D. Westmoreland, G. H. Allen, P. G. Bradley, T. J. Meyer and W. H. Wooddruff, *J. Am. Chem. Soc.*, 1984, **106**, 3492; (*b*) J. N. Demas and D. G. Taylor, *Inorg. Chem.*, 1979, **18**, 3177; (*c*) K. Mandal, T. D. L. Pearson, W. P. Krug and J. N. Demas, *J. Am. Chem. Soc.*, 1983, **105**, 701.
14 (*a*) J. V. Caspar and T. J. Meyer, *J. Am. Chem. Soc.*, 1983, **105**, 5583; (*b*) J. V. Caspar, B. P. Sullivan and T. J. Meyer, *Inorg. Chem.*, 1984, **23**, 2104.
15 V. Balzani, F. Bolletta and F. Scandola, *J. Am. Chem. Soc.*, 1980, **102**, 2552.
16 F. Scandola and V. Balzani, *J. Chem. Educ.*, 1983, **60**, 814.
17 F. Barigelletti, L. Flamigni, V. Balzani, J.-P. Collin, J.-P. Sauvage, A. Sour, E. C. Constable and A. M. W. C. Thompson, *J. Am. Chem. Soc.*, 1994, **116**, 7692.
18 C. K. Ryu and R. H. Schmehl, *J. Phys. Chem.*, 1989, **93**, 7961; L. De Cola, V. Balzani, F. Barigelletti, L. Flamigni, P. Belser, A. von Zelewsky, M. Frank and F. Vögtle, *Inorg. Chem.*, 1993, **32**, 5228.
19 N. Sutin, *Acc. Chem. Res.*, 1982, **15**, 275.
20 M. Furue, T. Yoshidzumi, S. Kinoshita, T. Kushida, S. Nozakura and M. Kamachi, *Bull. Chem. Soc. Jpn.*, 1991, **64**, 1632; R. H. Schmehl, R. A. Auerbach and W. F. Walcholtz, *J. Phys. Chem.*, 1988, **92**, 6202; R. H. Schmehl, R. A. Auerbach, W. F. Walcholtz and C. M. Elliott, *Inorg. Chem.*, 1986, **25**, 2440.
21 T. Föster, *Discuss. Faraday Soc.*, 1959, **27**, 7.
22 This distance, the midpoint between the Ru and Os centers, in **2e** is estimated using the space filling model in Insight/Discover of Biosym/MSI.
23 D. L. Dexter, *J. Chem. Phys.*, 1953, **21**, 836.
24 H. Schmidbaur and T. Pollok, *Angew. Chem.*, *Int. Ed. Engl.*, 1986, **25**, 348.
25 H. Schmidbaur, S. Manhart and A. Schier, *Chem. Ber.*, 1993, **126**, 2389.
26 I. J. Colquhoun and W. McFarlane, *J. Chem. Soc.*, *Dalton Trans.*, 1982, 1915.
27 D. A. Buckingham, F. P. Dwyer, H. A. Goodwin and A. M. Sargeson, *Aust. J. Chem.*, 1964, **17**, 325; E. M. Kober, J. V. Casper, B. P. Sullivan and T. J. Meyer, *Inorg. Chem.*, 1988, **27**, 4587.

*Received* 6*th April* 1998; *Paper* 8/02809E